DALTON
FULL PAPER

Bonding in mixed halogen and hydrogen peroxides

Adam J. Bridgeman* and Joanne Rothery

University Chemical Laboratories, Lensfield Road, Cambridge, UK CB2 1EW.
E-mail: ajb32@cam.ac.uk

Received 22nd June 1999, Accepted 24th September 1999

The geometries and vibrational frequencies of the hydrogen and halogen peroxides XOOX′ and the XOO and XO fragments (X, X′ = H, F, Cl, Br or I) have been studied using non-local density functional theory. The X–O, X′–O and O–O bond energies have been calculated and likely dissociation paths for these atmospherically important or potentially important molecules suggested. The sulfur analogues have also been examined. A unified model for these chemically diverse species is presented based on the interaction between O_2 and X · · · X fragments. The correlation between their electronic structures is outlined. The antibonding nature of the interaction between the halogen lone pairs and the π electrons of the O_2 fragments causes lengthening and weakening of the halogen–oxygen bonds. The electronegativity of X and X′ determines the extent and direction of the electron transfer between the O_2 and X · · · X fragments. The O–O bond order is thus sensitive to the nature of the substituents and the multiple bond character decreases steadily as the electronegativity of X and X′ decreases. The O–O bond strengths, though, are also affected by steric interactions between the halogen 'lone pairs'. The O–O bonds in the HO–OX′ species are thus much stronger than the bond orders and lengths suggest.

Halogen oxides are now known to play a significant role in the catalytic depletion of stratospheric ozone. Stratospheric chlorine atoms mainly result from the release of chlorofluorocarbons (CFCs) whilst the level of bromine is due to a variety of natural and man-made sources including organisms in sea water and solvents such as methyl bromide. The halogen atoms react with ozone removing oxygen atoms to form the halogen monoxides, eqn. (1). Molina and Molina[1] proposed the self-reaction of ClO

$$X + O_3 \longrightarrow XO + O_2 \qquad (1)$$

to form its dimer followed by subsequent reaction with ozone, eqns. (2). This has led to a number of experimental and theoretical studies[2,3] on the chemistry and physical properties of Cl_2O_2. It has been determined that the peroxide is the most stable isomeric form. The gas-phase structure has been determined from the rotational spectrum[2] and features long O–O and Cl–O bond lengths of 143 and 170 pm respectively. The O–O bond length should be contrasted with those in O_2F_2 (122 pm)[4] and H_2O_2 (148 pm).[5]

$$ClO + ClO + M \longrightarrow Cl_2O_2 + M \qquad (2a)$$

$$Cl_2O_2 + h\nu \longrightarrow 2Cl + O_2 \qquad (2b)$$

$$Cl + O_3 \longrightarrow ClO + O_2 \qquad (2c)$$

A number of experimental studies on the BrO self-reaction have also been reported[6] involving the short lived BrOOBr intermediate. The study by Yung *et al.*,[7] however, showed that the most effective ozone depleting cycle involving bromine is probably one in which BrO reacts with ClO, eqn. (3). Toohey

$$BrO + ClO \longrightarrow Br + Cl + O_2 \qquad (3)$$

and Anderson[8] proposed an intermediate [BrOOCl] to account for the observed reaction paths. As the OH radical is also present in the atmosphere, the analogous reactions of HO with ClO and BrO possibly through HOOX (X = Cl or Br) are also possible; HOOCl has been proposed[9] as an important stratospheric molecule.

Johnsson *et al.*[10] have used matrix isolation techniques to study the products of the reactions between Cl, Br and I atoms and ClO_2. These reactions yielded XOClO (X = Cl, Br or I) and were found to undergo photolytic transformations. No experimental studies of the reactions of FO or FO_2 with other halogens appear to have been reported.

The purpose of this study is to investigate the bond strengths, structures and vibrational spectra of the full set of mixed hydrogen and halogen peroxide molecules, XOOX′ (X, X′ = H, F, Cl, Br or I). A future paper will report calculations on the relative stabilities and bonding in the possible isomeric forms; peroxide XOOX′, chains XOX′O and X′OXO and the T-shaped $XX'(O)_2$ and $X'X(O)_2$. In addition to the studies on the $(ClO)_2$ dimer,[2] Guha and Francisco[11] have reported a detailed density functional study on the $XBrO_2$ (X = H, Cl or Br) isomers and Lee[12] has reported *ab initio* calculations on the possible fragmentation products.

As well as being important or potentially significant atmospheric species, these molecules present the possibility of studying the effects of substituent electronegativity on the electronic structure of the chemically widespread peroxide linkage. This paper also reports a model for the bonding in the XOOX′ species. The O–O bond lengths in HOOH, ClOOCl and FOOF are 148, 143 and 122 pm respectively[2,4,5] which should be compared to 121 pm in free O_2.

The bonding in FOOF has received considerable attention[13] as the O–O separation appears a severe test of the treatment of correlation by theoretical methods. In particular, these studies have been used to compare the accuracy of density functional (DF) methods with that of molecular orbital treatments. The performance of DF methods is, in general, found to be very good. This paper is concerned with the application of non-local DF calculations to the problem of the variation in the X–O, O–O and X′–O bond lengths, the torsional angle and the rotational barriers in the full set of XOOX′ (X, X′ = H, F, Cl, Br or I) molecules. A consistent level of theory using analogous basis sets is used throughout to reveal the underlining chemical

Table 1 Optimized structures of XOOX′ molecules (X, X′ = H, F, Cl, Br or I). The known experimental data are shown in parentheses. For comparison, r_{OO} for O_2 is 121 pm

	Bond length/pm			Bond angle/°			
XOOX′	r_{OO}	r_{OX}	$r_{OX'}$	θ_1	θ_2	τ	Ref.
HOOH	148 (149)	98 (97)	98 (97)	99 (95)	99 (95)	113 (111)	5
HOOF	138	99	153	103	107	84	
HOOCl	142	99	181	102	111	88	
HOOBr	142	99	196	102	111	89	
HOOI	144	99	210	102	114	94	
FOOF	122 (122)	161 (158)	161 (158)	111	111	89 (87)	4
FOOCl	125	161	194	110	116	87	
FOOBr	125	161	209	110	115	85	
FOOI	126	161	227	110	118	87	
ClOOCl	129 (143)	192 (170)	191 (170)	115	115	86 (81)	2
ClOOBr	128	192	207	114	115	85	
ClOOI	130	191	221	114	118	89	
BrOOBr	128	208	208	114	114	83	
BrOOI	131	207	221	114	118	87	
IOOI	133	220	219	119	118	88	

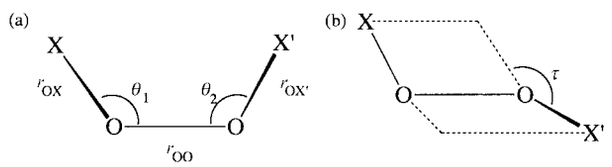

Fig. 1 Skewed structure of XOOX′ molecules and definitions of the (a) r_{OO}, r_{OX}, $r_{OX'}$, θ_1 and θ_2 and (b) τ internal coordinates.

variations. Burdett *et al.*[14] proposed a three-centre orbital model to rationalize the electronic structure of XOO systems in terms of the electronegativity of X and this was found to be more versatile than the (p–π*)σ model discussed by Jackson[15] and Spratley and Pimentel.[16]

Also of interest are the structures and bonding in the sulfur analogues, XSSX (X = H, F, Cl, Br or I). The S–S bond lengths are 205, 198, 197 and 189 pm in HSSH, BrSSBr, ClSSCl and FSSF.[17–19] These should be compared with the bond length of 189 pm in S_2 and indicate a similar variation in the S–S bond order with the electronegativity of X as observed in the peroxides.

Computational details

All density functional calculations were performed here using the 'DeFT' code written by St-Amant[20] in the linear combination of Gaussian-type orbitals (LCGTO) framework. The calculations set used the Vosko–Wilk–Nusair[21] local spin density (LSD) approximation of the correlation part of the exchange-correlation potential with non-local corrections using the Becke[22] functional for exchange and the Perdew[23] functional for correlation. The Gaussian basis sets (GTOs) and the auxiliary basis sets needed for the Coulomb and exchange potential were optimized specifically for LSD calculations by Godbout *et al.*;[24] GTO sets of double-ζ quality for the halogens and triple- and double-ζ quality for oxygen and sulfur were used. Bond orders were calculated from the density matrices according to the prescription suggested by Mayer.[25] Bond energies incorporate zero point energy corrections and refer to 0 K.

Results

(i) XOOX′

Fig. 1 shows a schematic view of the skewed structure of the XOOX′ species and the definition of the internal coordinates. Table 1 lists the optimized structure parameters together with experimental data, where available. Although the calculated

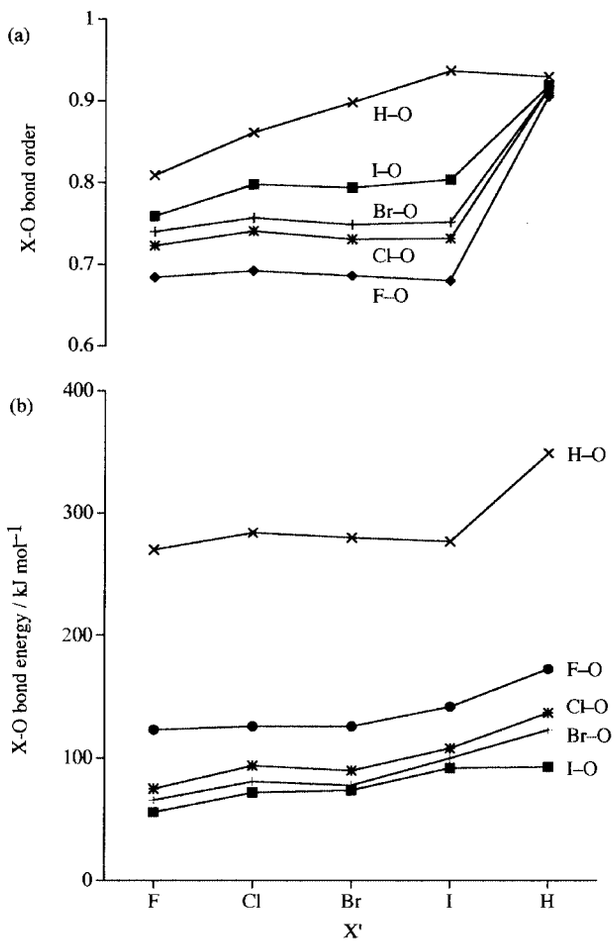

Fig. 2 Variation of (a) X–O bond order and (b) X–O bond energy (kJ mol^{-1}) with X′ in XOOX′ molecules. The bond energies were determined from the reaction XOOX′ ⟶ X + OOX′.

F–O and O–O bond lengths in FOOF are in excellent agreement with experiment, the agreement for ClOOCl is much poorer. Variation of the O and Cl basis sets made little difference to the optimized structure. Calculations at the LSD level led to an even shorter O–O separation so that the quality of the non-local correction appears to be key to the accuracy of the O–O binding. A similar result was reported by Guha and Francisco.[11] The calculated vibrational frequencies are listed in Table 2. Figs. 2 and 3 show the variation of the calculated X–OOX′ and XO–OX′ bond orders and energies respectively.

Table 2 Calculated vibrational bands (cm^{-1}) and approximate assignments for the XOOX′ species. The known experimental data are shown in parentheses. For comparison, the stretching frequency of O_2 is at 1555 cm^{-1}

XOOX′	OX stretch	OX′ stretch	OO stretch	XOO bend	OOX′ bend	Torsion
HOOH	3628 (3608)	3611 (3607)	1327 (1394)	1112 (1266)	895 (864)	388 (317)
HOOF	3493	977	1387	689	584	1387
HOOCl	3538	867	1352	572	478	1352
HOOBr	3545	865	1347	512	441	1347
HOOI	3551	819	1330	544	432	1330
FOOF	688 (630)	649 (614)	1307 (1210)	468 (466)	402 (360)	1307 (1210)
FOOCl	653	563	1191	434	311	1191
FOOBr	644	531	1208	434	281	1208
FOOI	621	433	1165	392	160	1165
ClOOCl	554 (679)	548 (633)	1055 (765)	362 (446)	273 (328)	1055 (765)
ClOOBr	550	515	1075	343	249	1075
ClOOI	535	432	997	319	218	997
BrOOBr	535	522	1071	306	237	1071
BrOOI	498	435	1009	286	209	1009
IOOI	452	437	920	273	202	920

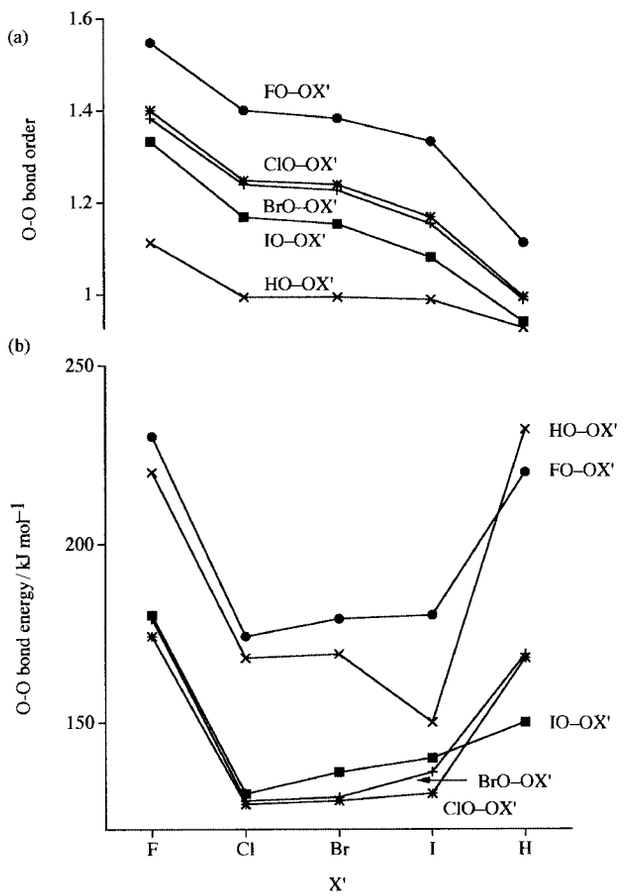

Fig. 3 Variation of (a) O–O bond order and (b) O–O bond energy (kJ mol^{-1}) with X and X′ in XOOX′ molecules. The bond energies were determined from the reaction XOOX′ ⟶ XO + OX′.

(ii) XOO and XO

Table 3 lists the optimized structural parameters and calculated bond orders for the XOO fragments together with experimental data, where available. It should be noted that the agreement with the experimental structures is much better than for ClOOCl. Table 4 lists the calculated vibrational frequencies together with experimental data, where available. Table 5 lists the structural parameters, bond orders and vibrational frequencies for the XO fragments together with the experimental data.

(iii) XSSX, XSS and XS

Table 6 lists the optimized structure parameters of the XSSX

Table 3 Optimized structures and calculated bond orders of XOO molecules (X = H, F, Cl, Br or I). The known experimental data are shown in parentheses. The values in italics are estimates

	Bond length/pm				Bond order	
XOO	r_{oo}	r_{ox}	θ_1/°	Ref.	O–O	O–X
HOO	136	99	104		1.36	0.90
FOO	122 (120)	165 (165)	112 (111)	26	1.22	0.63
ClOO	124 (123)	201 (183)	117 (110)	27	1.24	0.66
BrOO	124 (*125*)	215 (*200*)	118 (*115*)	28	1.24	0.67
IOO	124 (*125*)	243 (*240*)	117 (*120*)	29	1.24	0.63

Table 4 Calculated vibrational bands (cm^{-1}) and approximate assignments for the XOO species. The known experimental data are shown in parentheses. The values in italics are estimates

XOO	OX stretch	OO stretch	XOO bend	Ref.
HOO	3447 (3436)	1346 (1392)	1090 (1098)	30
FOO	646 (586)	1465 (1494)	395 (376)	26
ClOO	507 (432)	1378 (1441)	288 (215)	31
BrOO	525 (*250*)	1354 (*1487*)	243 (*160*)	32
IOO	414 (*275*)	1382 (*1500*)	193 (*150*)	29

Table 5 Optimized bond lengths (pm) and calculated vibrational bands (cm^{-1}) for the XO species. The known experimental data are shown in parentheses

XO	Bond length [33]	XO stretch [34]	Bond order
HO	99 (97)	3563 (3548)	0.94
FO	138 (136)	1071 (1029)	1.38
ClO	163 (157)	819 (780)	1.63
BrO	177 (172)	713 (723)	1.77
IO	194	640 (687)	1.94

together with experimental data, where available. The calculated vibrational frequencies are listed in Table 7. Tables 8 and 9 list the optimized structures and vibrational frequencies of the XSS and XS fragments. Fig. 4 shows the variation in the calculated X–SSX and XS–SX bond orders and energies.

Discussion

The energies and approximate descriptions of the molecular orbitals of FOOF, BrOOBr and HOOH are shown in Fig. 5. The orbitals of the C_2 systems can be generated by considering the interaction of the frontier orbitals of X · · · X with those of the O_2 molecule. The frontier orbitals of H · · · H are simply the a + b combinations of the 1s functions. The frontier orbitals of

Table 6 Optimized structures of XSSX molecules (X = H, F, Cl, Br or I). The known experimental data are shown in parentheses. For comparison, r_{SS} for S_2 is 189 pm

	Bond length/pm		Bond angle/°		
XSSX	r_{SS}	r_{SX}	θ_1	τ	Ref.
HSSH	209 (205)	135 (133)	98.6 (91)	91 (91)	17
FSSF	191 (189)	170 (164)	111 (108)	90 (88)	18
ClSSCl	193 (197)	211 (207)	110 (108)	86 (85)	19
BrSSBr	194 (198)	226 (224)	109 (109)	84 (84)	19
ISSI	196	248	111	86	

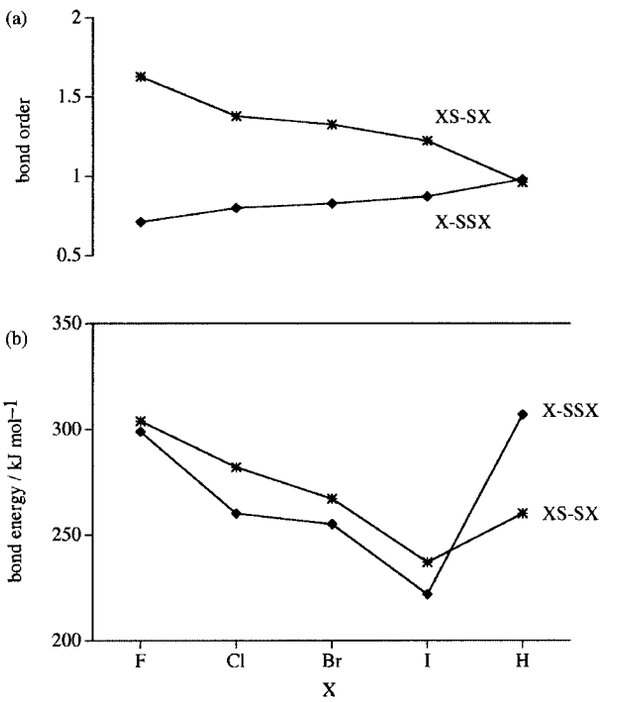

Fig. 4 Variation of (a) S–S and S–X bond order and (b) S–S and S–X bond energy (kJ mol^{-1}) with X in XSSX molecules. The bond energies were determined from the reactions XSSX ⟶ 2XS and XSSX ⟶ X + SSX.

F···F and Br···Br are combinations of their valence p functions.

Thus, 1a is derived from the $2p\sigma_g$ function of O_2 and is X–O–O–X bonding. Similarly, 1b and 2a correlate with the $2p\pi_u$ functions of O_2. The higher electronegativity of fluorine and bromine leads to better interaction with the quite low lying $2p\pi_u$ orbitals. The energies of 1b and 2a in these XOOX molecules decrease with the electronegativity of X. Orbital 2a does not contribute to the H–O bonding in HOOH. There is some rehybridization on oxygen to increase the O–H bonding in 1a at the expense of reducing the O–O π-type interaction in 2a.

The orbitals 2b and 3a derive from the bonding overlap of X···X functions with the O_2 $2p\pi_g$ orbitals. These are the highest occupied levels of HOOH so that the O–O π-type bonding is effectively destroyed. As shown in Figs. 2 and 3, the H–O and O–O bond orders are both close to unity. The Mulliken charges of O and H are calculated to be −0.31 and +0.31 which can be interpreted to be the result of donation of electron density from H to the $2p\pi_g$ orbitals of O_2 with the resulting decrease in O–O bond order. Resonance form **2** in Scheme 1 is of considerable importance.

The 2b and 3a functions in FOOF and BrOOBr are similar to those in HOOH. The high electronegativity of fluorine results in transfer of electron density from oxygen and considerable stabilization of this O–O antibonding function.

The 3b and 4a functions in FOOF and BrOOBr are halogen-based, non-bonding 'lone pairs'. The higher electronegativity of fluorine, as outlined above, leads to greater bonding interaction between the F 2p and O_2 $2p\pi_u$ functions resulting in the low energy of 2a and 1b. It similarly leads to the relatively low energy of the corresponding antibonding functions which are 4b and 5a in FOOF. As shown in Fig. 4, these are F–O *anti*-bonding but O–O bonding. These are the highest occupied orbitals in FOOF with the result that the F–O bond order is considerably reduced but the O–O bond is maintained.

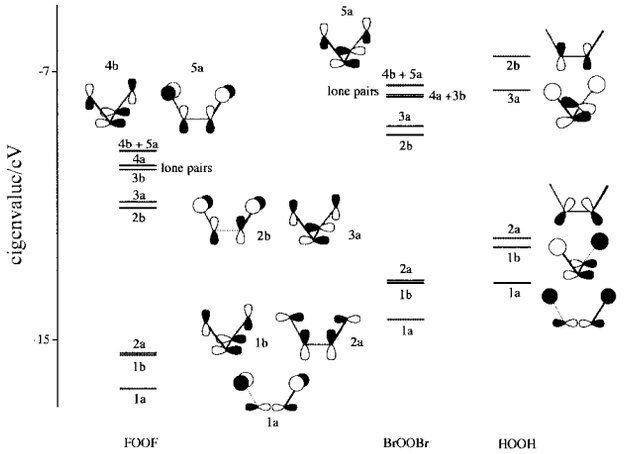

Fig. 5 Energies and approximate descriptions of the occupied molecular orbitals of FOOF, BrOOBr and HOOH. The low lying, core and valence s functions have been omitted.

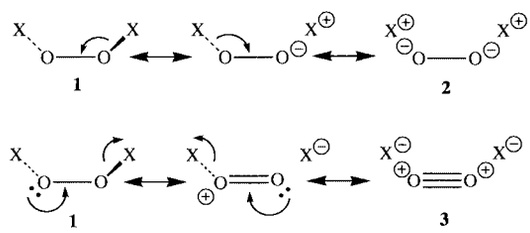

Scheme 1

In FOOF there is effectively a 4-orbital, 8-electron interaction between the p orbitals of F···F and the $2p\pi_u$ functions of O_2 resulting in weak F–O bonds and little *net* transfer of charge. It is primarily this repulsive interaction which causes the long F–O bond. There is some bonding interaction with the $2p\sigma_g$ and $2p\pi_g$ functions of O_2. The latter results in a O→F charge transfer and a degree of strengthening of the O–O bonds. The calculated Mulliken charges are −0.19 and +0.19 for fluorine and oxygen respectively. The electronegative fluorine acts to reduce the π* electron density in the O–O bond. Resonance form **3** in Scheme 1 is of considerable importance.

Calculations were also performed in FOOF with the F–O bonds shortened to 140.5 pm (the value observed[38] in OF_2) and the O–O bond lengthened to 148.0 pm (the value observed[5] in HOOH). This led to an increase in energy for the orbitals 1a, 1b, 2a, 4b and 5a which are all O–O bonding. The O–O antibonding functions, 2b and 3a, are considerably stabilized. The fluorine 'lone pair' orbitals, 3b and 4a, are also significantly stabilized indicating the importance of the steric interaction between the halogen atoms.

The lower electronegativity of bromine leads to a smaller interaction with the $2p\pi_u$ orbitals of O_2 but a *larger* interaction with $2p\pi_g$. The 4b function of BrOOBr is effectively a non-bonding orbital. The highest occupied orbital of BrOOBr is 5a which derives from one of the $2p\pi_g$ functions of O_2. It is antibonding between all the connected atoms. The bonding scheme is thus intermediate between the cases for HOOH and FOOF and the calculated Mulliken charges are +0.02 and −0.02 for bromine and oxygen respectively. The uncharged resonance form **1** is thus an appropriate description of the bonding.

Table 7 Calculated vibrational bands (cm^{-1}) and approximate assignments for the XSSX species. The known experimental data are shown in parentheses. For comparison, the stretching frequency of S_2 is 623 cm^{-1}

XSSX	SX sym stretch	SX asym stretch	SS stretch	XSS bend	SSX bend	Torsion
HSSH	2606 (2480)	2613 (2495)	491 (501)	859 (868)	729 (868)	427
FSSF	593 (718)	588 (684)	556 (526)	250	280 (333)	123
ClSSCl	416 (446)	433 (434)	568 (540)	200 (205)	230 (238)	88 (102)
BrSSBr	350 (356)	362 (353)	557 (534)	170 (171)	194 (200)	56 (68)
ISSI	304	308	534	138	163	27

Table 8 Optimized structures and vibrational bands (cm^{-1}) for XSS species (X = H, F, Cl, Br or I)

	Bond length/pm			Vibrational band		
XSS	r_{SS}	r_{SX}	θ_1/°	XS stretch	SS stretch	XSS bend
HSS	200	137	103	2511	550	874
FSS	170	191	110	566	655	261
ClSS	213	190	112	416	663	209
BrSS	228	191	112	344	658	170
ISS	251	191	114	291	647	142

Table 9 Optimized bond lengths (pm) and vibrational bands (cm^{-1}) for XS species (X = H, F, Cl, Br or I) together with experimental data in parentheses

XS	Bond length/pm	Ref.	Vibrational band	Ref.
HS	135 (134)	35	2648 (2591)	36
FS	163		771	
ClS	200		557 (617)	37
BrS	214		467 (518)	37
IS	233		427 (443)	37

In the mixed peroxides XOOX′ the Mulliken charges follow predictable patterns. In all the HOOX′ (X′ = F, Cl, Br or I) species there is calculated to be overall transfer of charge to the O_2 fragment and for this to increase as the electronegativity of X′ decreases. In all the fluorides *except* HOOF there is overall removal of charge from the O_2 unit. In the mixed chlorine, bromine and iodine species there is overall transfer of charge to O_2.

The lack of symmetry in the XOOX′ (X ≠ X′) peroxides leads to extensive mixing of the valence orbitals and a simple analysis of the molecular orbitals is not possible. In the FOOX′ (X′ Cl, Br or I) systems the lowest orbitals are more F in character whilst the highest are essentially X′ lone pairs. Increasing donation of electron density by the less electronegative X′ allows rehybridization of the oxygen atoms to minimize the F–O antibonding interactions observed in FOOF. The rehybridization of the oxygen atoms reduces the 'π-type' interaction of the O_2 fragment. Thus, as shown in Figs. 2 and 3, the F–O bond order and strength increase whilst the O–O bond order decreases as the electronegativity of X′ decreases. Similar patterns are observed for the chlorine, bromine and iodine species. The X–O bond strength decreases in the series H–O > F–O > Cl–O > Br–O > I–O, in the same order as the bond length variation.

The O–O bond strength follows a more complex pattern and does not mirror the bond order curve. The shortness of the O–O bond in the XOOX′ (X, X′ = F, Cl, Br or I) species is due to the small degree of electron transfer to the O_2 fragment and results in a high O–O bond order. It also leads to considerable steric repulsion between X and X′. As the electronegativity of X′ is lowered, the increased X′→O_2 donation lengthens the O–O bond and reduces the bond order. The strongest O–O bonds in the XOOX′ (X, X′ = F, Cl, Br or I) molecules are thus found in those containing fluorine.

The O–O bonds in the XOOH species are amongst the strongest despite these having the smallest bond order for each X. In the HOOX′ species the electron transfer by hydrogen lengthens the O–O considerably and this is reflected in the bond orders which are close to one for X = Cl, Br or I. The strength of the bond appears to result from the lack of X/X′ lone-pair/lone-pair repulsions in the species.

The ground states of the XO and XOO systems are all $^2\Pi$ and $^2A''$ respectively. In both the XO and XOO fragments the unpaired electron is housed in a π* orbital which varies in character with the electronegativity of X. In FO, for example, the spin density is 85% on the less electronegative oxygen atom. In IO, however, the oxygen spin density is reduced to around 66%. Although HO contains the least electronegative X atom, the unpaired electron is housed in a non-bonding oxygen p orbital.

As shown in Table 1, all the XOOX′ peroxides adopt the skewed structure shown in Fig. 1 with torsion angles quite close to 90°. The barrier to rotation of HOOH is calculated to be *ca.* 37 kJ mol^{-1} for rotation *via* the *cis* form and *ca.* 5 kJ mol^{-1} for rotation *via* the *trans* form. The barriers are considerably higher in the halogen peroxides (for example, the *cis* and *trans* barriers are 134 and 124 kJ mol^{-1} respectively for FOOF and 162 and 155 kJ mol^{-1} respectively for FOOI). The source of the barrier can be clearly seen in Fig. 5. In the planar forms a p orbital on each oxygen lies perpendicular to the molecular plane and cannot interact appreciably with the X σ orbitals. The *cis*-planar form maximizes the steric interactions between the halogen lone pairs and due to the short O–O bonds this becomes highly destabilizing. Constraining HOOH to be linear leads to dissociation into 2 OH fragments.

The bonding in XSSX is very similar to that in the peroxides. The lower electronegativity of sulfur leads to net transfer of charge to the S_2 fragment for X = F, Cl, Br or I. In FSSF the Mulliken charges are −0.34 and +0.34 for fluorine and sulfur respectively. The molecular orbital scheme is very similar to that pictured in Fig. 5 for FOOF. As outlined above, the interaction of the fluorine p orbitals with the $2p\pi_u$ functions of the O_2 fragment leads to a net repulsive interaction weakening the F–O bond. The F–O bond length of 158 pm is considerably longer than that in OF_2 (148 pm). The longer S–F bond acts to decrease the orbital overlap so that this repulsive interaction is reduced. The S–F bond length is observed to be 164 pm which is also longer than that for SF_2 (159 pm) but the difference is much smaller and the bond length does not appear anomalous. The S–X bonds (X = F, Cl, Br or I) are predicted to be *stronger* than the analogous O–X bonds.

The lower electronegativity of sulfur leads to greater removal of electron density from the $3p\pi_g$ orbitals of the S_2 fragment in all the halides than in the peroxide species. As shown in Table 6 and Fig. 5, the S–S bond order and length indicates multiple bond character in each species. Decreased electron removal by the less electronegative X leads to a lower S–S bond order. The S–S bond strengths mirror the bond orders. The effect of the steric repulsion between the X atoms is less apparent than in the peroxides, due to the longer S–S separation, although the HS–SH bond is stronger than the bond order would suggest.

Conclusion

Density functional calculations have been used to predict the structures, vibrational spectra and to rationalize the bonding in XOOX′ and XSSX (X, X′ = F, Cl, Br, I or H). In the halogen and mixed halogen peroxides the bond energies indicate that dissociation of the XOOX′ molecules is likely to produce the heavier halogen atom and an XOO radical. In the HOOX′ species dissociation to produce HO and X′O is likely to be thermodynamically favoured. In the XSSX molecules the X–S and S–S bond strengths are similar.

The observed and calculated structural trends can be rationalized by analysis of the key orbital interactions. The bonding models discussed previously by Burdett *et al.*,[14] Jackson[15] and Spratley and Pimentel[16] have been enlarged. Both approaches concentrate on the interaction between a σ-type hybrid on X with the π orbitals of the O_2 fragment. In all the species studied, however, a significant part of the bonding interaction results from the interaction with the $2p\sigma_g$ orbital of the O_2 fragment. In addition, the halogen atoms do not interact through purely σ-type interactions and all of their p electrons have to be considered.

The anomalously long F–O bond in FOOF appears to result from the repulsive interaction with the $2p\pi_u$ functions of O_2 and the relatively small bonding interaction with the $2p\pi_g$ orbitals. The former can be described as a steric repulsion between fluorine 'lone pairs' and the O_2 π bonds. This is reduced in importance for the systems containing the larger halogen atoms and, of course, does not occur in HOOH.

The steric repulsion between the X/X′ 'lone pairs' is also significant, particularly due to the rather short XO–OX′ separations. Thus, although there is considerable O–O multiple bond character in the XOOX′ (X, X′ ≠ F or H) species, the bond is weaker than the single bond in HOOH.

The Burdett *et al.*[14] approach describes well the qualititative effect of the electronegativity of X on the O–O bond order. The present set of molecules allows this to be quantified for a series with a range of structures. The more electronegative substituents act to withdraw electron density from the π orbitals of the O_2 fragment whilst the less electronegative groups lead to increased electron density in the O_2 π* orbitals. This causes rehybridization of the oxygen orbitals to minimize the antibonding interaction and maximize the O–X bonding.

Acknowledgements

The authors would like to thank Dr Alain St-Amant of the University of Ottawa for making the DeFT code publicly available. J. R. acknowledges the receipt of an EPSRC studentship and Trinity College, Cambridge for financial support.

References

1 L. T. Molina and M. J. Molina, *J. Phys. Chem.*, 1987, **91**, 433.
2 M. Birk, R. R. Friedl, E. A. Cohen, H. M. Pickett and S. P. Sander, *J. Chem. Phys.*, 1989, **91**, 6588.
3 M. P. McGrath, K. C. Clemitshaw, F. S. Rowland and W. J. Hehre, *J. Phys. Chem.*, 1990, **94**, 6126; F. Jensen and J. Oddershede, *J. Phys. Chem.*, 1990, **94**, 2235; J. B. Burkholder, J. J. Orlando and C. J. Howard, *J. Phys. Chem.*, 1990, **94**, 687; M. J. Molina, A. J. Colussi, L. T. Molina, R. N. Schindler and T. L. Tso, *Chem. Phys. Lett.*, 1990, **173**, 310; I. J. Eberstein, *J. Geophys. Res. Lett.*, 1990, **17**, 721; W. B. DeMore and E. Tschuikow-Roux, *J. Phys. Chem.*, 1990, **94**, 5556; S. Abramowitz and M. W. Chase, Jr., *Pure Appl. Chem.*, 1991, **63**, 1449; J. Jacobs, M. Kronberg, H. S. P. Müller and H. Willner, *J. Am. Chem. Soc.*, 1994, **116**, 1106; K. J. Huder and W. B. DeMore, *J. Phys. Chem.*, 1995, **99**, 3905; M. Schwell, H.-W. Jochims, B. Wassermann, U. Rockland, R. Flesch and E. Rühl, *J. Phys. Chem.*, 1996, **100**, 10070; W.-K. Li and C.-Y. Ng, *J. Phys. Chem.*, 1997, **101**, 113.
4 R. H. Jackson, *J. Chem. Soc.*, 1962, 4585.
5 R. L. Redington, W. B. Olsen and P. C. Cross, *J. Chem. Phys.*, 1962, **36**, 7311.
6 M. A. Clyde and J. A. Coxon, *Proc. R. Soc. London*, *Ser. A*, 1968, **303**, 207; N. Basco and S. K. Dogra, *Proc. R. Soc. London*, *Ser. A*, 1971, **333**, 41; M. A. Clyde and R. T. Watson, *J. Chem. Soc.*, *Faraday Trans.*, 1975, 336; S. P. Sander and R. T. Watson, *J. Phys. Chem.*, 1981, **85**, 4000.
7 Y. L. Yung, J. P. Pinto, R. T. Watson and S. P. Sander, *J. Atmos. Sci.*, 1980, **37**, 339.
8 D. W. Toohey and J. G. Anderson, *J. Phys. Chem.*, 1988, **92**, 1705.
9 J. S. Francisco, S. P. Sander, T. J. Lee and A. P. Rendell, *J. Phys. Chem.*, 1994, **98**, 5644.
10 K. Johnsson, A. Engdahl, J. Kölm, J. Nieminen and B. Nelander, *J. Phys. Chem.*, 1995, **99**, 3902.
11 S. Guha and J. S. Francisco, *J. Phys. Chem.*, 1997, **101**, 5347.
12 T. J. Lee, *J. Phys. Chem.*, 1995, **99**, 15074.
13 D. A. Clabo and H. F. Schäffer, *Int. J. Quantum Chem.*, 1987, **31**, 429; D. A. Dixon, J. Andzelm, G. Fitzgerald and E. Wimmer, *J. Phys. Chem.*, 1991, **95**, 9197; R. D. Amos, C. W. Murray and N. C. Handy, *Chem. Phys. Lett.*, 1993, **202**, 489; B. S. Jursic, *Theochem-J. Mol. Struct.*, 1996, **366**, 97; O. N. Ventura, R. E. Cachau and M. Kieninger, *Chem. Phys. Lett.*, 1999, **301**, 331; O. N. Ventura, M. Kieninger and R. E. Cachau, *J. Phys. Chem.*, 1999, **103**, 147; B. S. Jursic, *Theochem-J. Mol. Struct.*, 1999, **459**, 23.
14 J. K. Burdett, N. J. Lawrence and J. J. Turner, *Inorg. Chem.*, 1984, **23**, 2419.
15 R. H. Jackson, *J. Chem. Soc.*, 1962, 4585.
16 R. D. Spratley and G. C. Pimentel, *J. Am. Chem. Soc.*, 1966, **88**, 2394.
17 D. P. Stevenson and J. Y. Beach, *J. Am. Chem. Soc.*, 1932, **60**, 2872.
18 R. L. Kuczkowski, *J. Am. Chem. Soc.*, 1964, **86**, 3617.
19 E. Hirota, *Bull. Chem. Soc. Jpn.*, 1958, **31**, 130; R. Kneip, L. Korte and D. Mootz, *Z. Naturforsch. B*, *Anorg. Chem. Org. Chem.*, 1983, **38**, 1.
20 A. St-Amant, DeFT, a FORTRAN program, University of Ottawa, 1994.
21 S. H. Vosko, L. Wilk and M. Nusair, *Can. J. Phys.*, 1980, **58**, 1200.
22 A. D. Becke, *Phys. Rev. A*, 1988, **38**, 3098.
23 J. P. Perdew, *Phys. Rev. B*, 1986, **33**, 8822.
24 N. Godbout, D. R. Salahub, J. Andzelm and E. Wimmer, *Can. J. Chem.*, 1992, **70**, 1992.
25 I. Mayer, *Chem. Phys. Lett.*, 1983, **97**, 270; *Int. J. Quantum Chem.*, 1984, **26**, 151.
26 R. D. Spratley, G. C. Pimentel and J. J. Turner, *J. Chem. Phys.*, 1966, **44**, 2063.
27 J. Troe, *J. Chem. Phys.*, 1991, **95**, 6483.
28 N. I. Butkovskaya, I. I. Morozov, V. L. Talrose and E. S. Vasiliev, *Chem. Phys.*, 1983, **79**, 21.
29 M. W. Chase, *J. Phys. Chem. Ref. Data*, 1996, **25**, 1323.
30 H. Uehara, K. Kawaguchi and E. Hirota, *J. Chem. Phys.*, 1985, **83**, 5479.
31 H. S. P. Muller and H. Willner, *J. Phys. Chem.*, 1993, **97**, 10589.
32 M. E. Jacox, *J. Phys. Chem. Ref. Data*, 1994, **3**, 461.
33 A. I. Bolydrev and J. Simons, *Periodic Table of Diatomic Molecules*, Wiley, New York, 1997.
34 G. Herzberg, *Spectra of Diatomic Molecules*, Van Nostrand-Reinhold, New York, 1950.
35 D. A. Ramsay, *J. Chem. Phys.*, 1952, **20**, 1920.
36 C. M. Pathak and H. B. Palmer, *J. Mol. Spectrosc.*, 1969, **32**, 157.
37 N. Acquista and L. J. Schoen, *J. Chem. Phys.*, 1970, **53**, 1290.
38 S. Abramowitz and M. W. Chase, *Pure Appl. Chem.*, 1991, **63**.

Paper 9/04968A